

# INERTIAL FORCES REPRODUCE THE OBSERVED VARIATIONS OF THE FREQUENCY OF GEOMAGNETIC REVERSALS

**KLAUDIO PEQINI**

Department of Physics, Faculty of Natural Sciences,  
University of Tirana, Albania

Corresponding author: Klaudio Peqini  
e-mail: [klaudio.peqini@fshn.edu.al](mailto:klaudio.peqini@fshn.edu.al)

---

## ABSTRACT

Understanding the geodynamo is a complex endeavor that heavily relies on advanced numerical modeling. Current magnetohydrodynamic (MHD) models, designed to replicate its behavior, operate within parameter regimes that are significantly removed from the estimated conditions in Earth's outer core. Despite their sophistication, these models often fail to reproduce magnetic fields that closely resemble those of the Earth and demand substantial computational resources. This paper focuses on the polarity reversal record, which is marked by a distinct change in the frequency of reversals over geological timescales. MHD models, due to their inherent complexity, offer limited insight into the underlying causes of these observational patterns. As an alternative, the domino model emerges as a computationally efficient tool capable of capturing many essential features of the main dipolar magnetic field. In this study, we analyze two versions of the domino model: one that incorporates inertial forces and a diffusive version. Although both versions share a similar reversal mechanism, the structure of their differential equations suggests that they operate within different dynamical regimes. Notably, the inertial version of the domino model generates a polarity reversal record that closely mirrors that observed in nature. We further explore potential extensions of the inertial domino model by incorporating additional mechanisms relevant to the dynamics of Earth's outer core. These enhancements aim to transform the model into a more comprehensive and effective framework. The insights gained from this simplified yet informative approach may ultimately contribute to refining the full-scale magnetohydrodynamic models of the geodynamo.

**Keywords:** Geodynamo, low-dimensional models, domino model, dipolar field reversals, dipolar moment

## 1. INTRODUCTION

Magnetic fields are present around a wide range of astrophysical bodies, including planets, stars, planetary nebulae, supernova remnants (such as magnetars), and even galaxies (Davidson 2013a). These fields constitute complex systems that exhibit a diverse array of topologies and spatiotemporal evolutions. Among them, Earth's magnetic field—also known as the geomagnetic field—is the most thoroughly studied (Backus *et al.*, 1996). Extensive datasets exist, comprising both direct measurements and historical records, which span multiple temporal and spatial scales ranging from thousands to millions of years (Valet *et al.*, 2006; Guyodo and Valet, 2006).

The geodynamo is a remarkably complex system characterized by rich and dynamic behavior. As heat escapes from the inner core and is transferred outward, it drives thermal and buoyant convective motion: hotter, less dense fluid rises, while cooler, denser fluid sinks. Simultaneously, Earth's rotation imposes Coriolis forces that organize these convective flows into helical, columnar structures (Busse 1975; Kageyama and Sato 1997). The motion of this electrically conductive fluid through an existing magnetic field induces electric currents, which, according to the induction equation, generate additional magnetic fields (Backus *et al.*, 1996; Duka *et al.*, 2015). This self-sustaining process, in which fluid motion reinforces the magnetic field, forms the essence of the dynamo mechanism (Roberts and King 2013). Turbulent convection in the liquid outer core plays a critical role. The chaotic and turbulent nature of the flow—coupled with the complex interplay among convection, rotation, and magnetism—gives rise to the intricate and continually evolving structure of Earth's magnetic field, including its periodic reversals (Spence *et al.*, 2006).

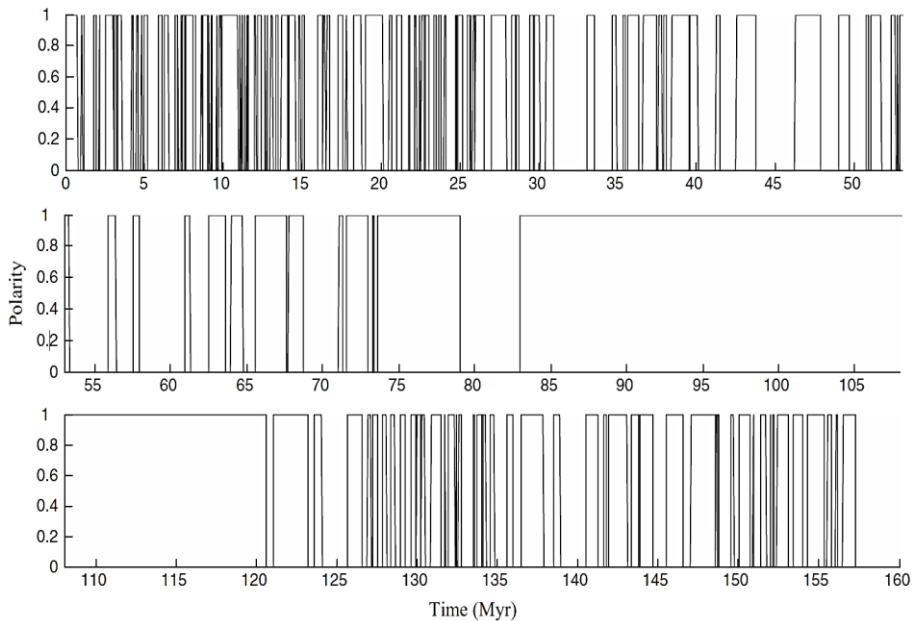


**Fig. 1** The time series of the polarity reversals for the period of 157.5 Myr provided by Cande and Kent (1992). There it is shown the polarity of the Dipolar field for the last 157.5 million years. The time “0” refers to the present (adapted from Duka *et al.*, 2015).

On Earth’s surface, approximately 90% of the total magnetic field (Backus *et al.*, 1996) closely resembles that of a giant bar magnet tilted at a variable angle relative to the planet’s rotational axis. This configuration, known as the dipolar field, is far from stable—it has undergone numerous polarity reversals throughout Earth’s history. Over geological time, the dipolar field has flipped, meaning the magnetic North and South poles have switched places. These geomagnetic reversals occur intermittently, with an average frequency of approximately every 200,000 to 300,000 years, though with significant variability (Guyodo and Valet 2006; Olson *et al.*, 2010; Mori *et al.*, 2013; Duka *et al.*, 2015; Peqini *et al.*, 2015; Valet and Fournier 2016; Raphaldini *et al.*, 2021). This irregularity is clearly illustrated in Figure 1, which shows the dipolar field’s polarity over the past 157.5 million years. Periods of frequent reversals are interspersed with intervals of prolonged stability, lasting tens of millions of years (Cande and Kent 1992; Valet and Fournier 2016; Raphaldini *et al.*, 2021). Such variability suggests changes in the underlying behavior of the geodynamo

over time (Carbone *et al.*, 2020). Several studies have proposed that variations in heat flux across the core–mantle boundary (CMB) may influence the frequency of geomagnetic reversals. Notably, efforts have been made to quantify how changes in the amplitude of CMB heat flux affect reversal rates (Olson *et al.*, 2010; Olson *et al.*, 2014). However, deriving clear insights and interpretations within the framework of magnetohydrodynamic (MHD) models remains a significant challenge.

Fortunately, an alternative approach exists: rather than relying on computationally intensive magnetohydrodynamic (MHD) models, one can construct simpler low-dimensional models that focus on specific aspects of the system, such as dipolar field reversals. In this paper, we briefly review the *domino model* and analyze two versions of it, originally proposed to yield similar results (Nakamichi *et al.*, 2012). Despite its structural simplicity and extremely low computational cost, the domino model appears to be well-designed for capturing reversals and other temporal variations of the dipolar geomagnetic field (see below for details and references). Moreover, it offers a promising framework for the development of more refined models that may contribute to a deeper understanding of geomagnetic field dynamics.

The structure of the paper is as follows: Section 2 presents the theoretical framework of the domino model, focusing on two specific versions. Section 3 outlines the corresponding results, while Section 4 offers an in-depth discussion of potential directions for extending the model. Finally, Section 5 concludes the paper by summarizing the main findings.

## 2. Domino model: Motivations and Theoretical Framework

Early simulations using full magnetohydrodynamic (MHD) models have shown that, in the convection-driven regime, striking columnar structures emerge within the liquid outer core (Kageyama and Sato 1997). Such structures are both theoretically expected and commonly observed in rapidly rotating, low-viscosity fluids, as described by the Proudman–Taylor theorem (Backus *et al.*, 1996; Davidson 2013b; Duka *et al.*, 2015; Peqini *et al.*, 2015). These columnar structures generate their own magnetic fields, and their cumulative effect constitutes a significant portion of the internally generated dipolar magnetic field. This concept forms the foundational assumption of the domino model (see Fig. 2). Each column is in rotational motion, characterized by the angle  $\theta_i$ , which denotes

the orientation of the column's axis relative to Earth's rotation axis. According to the Proudman–Taylor theorem, columns have a natural tendency to align with the rotation axis, resulting in a restoring force that opposes large deviations in orientation. The magnetic fields generated by individual columns interact with one another, and these interactions are modeled using an Ising-like spin framework. Additionally, the columns experience drag forces due to the viscous properties of the outer core, modeled as being proportional to their angular velocity. Finally, the columns are subjected to random external forces that emulate the effect of heat flow originating at the boundary between the inner and outer core.

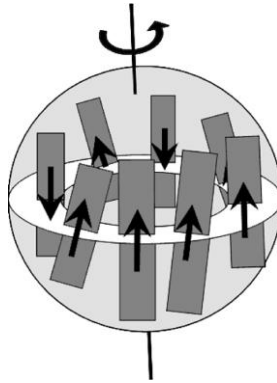


**Fig. 2** Sketch of the domino model, adapted from Duka *et al.*, 2015.

The primary motivation for developing the domino model is the explanation it provides for dipolar geomagnetic reversals—intermittent changes in the orientation of the dipolar geomagnetic field (Guyodo and Valet 2006; Kuipers *et al.*, 2009; Olson *et al.*, 2010; Valet and Fournier 2016). While these authors analyze various aspects of reversals, they do not offer an intuitive description of the underlying reversal mechanism. In contrast, the domino model presents a straightforward and conceptually clear explanation.

The assumptions and concepts outlined above can be summarized in the following Lagrangian formulation (Nakamichi *et al.*, 2012; Mori *et al.*, 2013; Duka *et al.*, 2015; Pegini *et al.*, 2015):

$$L = \frac{1}{2} \sum_{i=1}^N \frac{d\theta_i}{dt} - \gamma \sum_{i=1}^N (\boldsymbol{\Omega} \cdot \mathbf{S}_i)^2 - \lambda \sum_{i=1}^N \mathbf{S}_i \cdot \mathbf{S}_{i+1} \quad (1)$$

Here,  $N$  denotes the number of spins,  $S_i$ , which serve as free parameters. Each spin represents the magnetic field generated by its corresponding convective column. The first term models the kinetic energy of each column/spin, while the remaining terms capture the tendency of spins to align with the rotation axis and the spin-like interactions between the magnetic fields of neighboring columns. Notably, the  $\Omega \cdot S_i$  term is squared, reflecting the symmetry between upward and downward orientations and thereby mimicking the symmetry found in magnetohydrodynamic models (Mori *et al.*, 2013; Duka *et al.*, 2015; Peqini *et al.*, 2015). The free parameters  $\gamma$  and  $\lambda$  must be negative to ensure attractive interactions. The Lagrangian (1) is then subjected to a modified set of Euler–Lagrange equations that incorporate drag and random forcing terms (Duka *et al.*, 2015; Peqini *et al.*, 2015):

$$\frac{d}{dt} \left( \frac{\partial L}{\partial(d\theta_i/dt)} \right) = \frac{\partial L}{\partial\theta_i} - \kappa \frac{d\theta_i}{dt} + \frac{\varepsilon\chi_i}{\sqrt{\tau}} \quad (2)$$

Here  $\kappa$ ,  $\varepsilon$  and  $\chi_i$  denote the drag coefficient, the magnitude of the random forcing, and a random variable drawn from a normal distribution with zero mean and unit variance, respectively (Mori *et al.*, 2013; Duka *et al.*, 2015). Additionally,  $\tau$  is a parameter chosen to be a measure for the time step in the numerical procedure.

By applying straightforward calculations involving partial and total time derivatives, the following set of  $N$  equations is obtained:

$$\frac{d^2\theta_i}{dt^2} = \gamma \sin 2\theta_i - \lambda [\cos \theta_i (\sin \theta_{i-1} + \sin \theta_{i+1}) - \sin \theta_i (\cos \theta_{i-1} + \cos \theta_{i+1})] - \kappa \frac{d\theta_i}{dt} + \frac{\varepsilon\chi_i}{\sqrt{\tau}} \quad (3)$$

Periodic boundary conditions are employed in the model (Duka *et al.*, 2015) for several important reasons. The Earth’s magnetic field is generated by convective flows in the liquid outer core, which are inherently cyclic and continuous in space. Moreover, the core lacks rigid boundaries—unlike a confined box—where magnetic field lines abruptly terminate; instead, magnetic flux is continuously transported and regenerated throughout the fluid. In a finite, non-periodic system, spins located at the edges would behave differently from those in the interior,

potentially introducing unwanted artifacts. The use of periodic boundary conditions ensures that every spin experiences identical surroundings, thereby eliminating edge effects that could distort the dynamics of geomagnetic reversals.

### 3. RESULTS

The domino model (3) involves five free parameters, or hyperparameters:  $N$ ,  $\gamma$ ,  $\lambda$ ,  $\kappa$ . Variations in any of these parameters can have significant impacts on the model's output time series. The parameter space and regions of interest have been explored in previous studies (Mori *et al.*, 2013; Duka *et al.*, 2015), though a detailed discussion is beyond the scope of this paper. The second-order ordinary differential equations (ODEs) in equation (4) are solved numerically using a standard fourth-order Runge–Kutta method. Unlike the forward Euler method, which is highly sensitive to the choice of time step, the Runge–Kutta algorithm is considerably more stable and robust (Mori *et al.*, 2013; Peqini *et al.*, 2015).

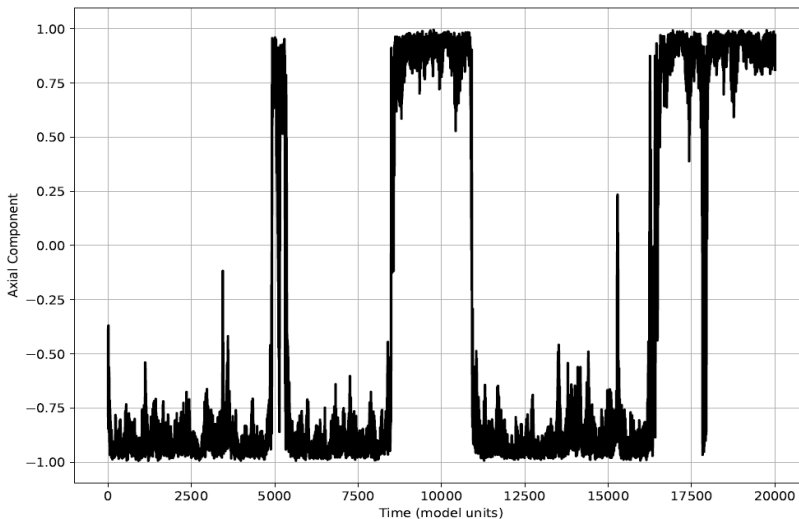


**Fig. 3** Typical time series generated by the domino model (3). The time scale is in the model's time units.

The output of the domino model equations (3) is the axial component, referred to as the magnetization (see Fig. 3). This component is computed by summing the axial components of all spins. A maximum value of +1

(or a minimum of  $-1$ ) corresponds to complete alignment in the positive (or opposite) direction. The resulting time series exhibits complex behavior and can be generated for arbitrary durations. Time is typically expressed in model units, calculated as described in Duka *et al.*, (2015).

The domino model's depiction of continuous and irregular axial oscillations of the dipolar moment can be linked to various geomagnetic phenomena observed in paleomagnetic records. The short-term oscillations in the dipole moment, resulting from fluctuations of individual spins, resemble secular variation. This term refers to gradual changes in the Earth's magnetic field over years to centuries, reflecting the dynamic nature of the geodynamo and providing insights into fluid motions within the Earth's outer core (Buffett 2024). Larger intensity fluctuations in the model, interpreted as intermittent large rotations of multiple spins, correspond to geomagnetic excursions. Excursions are temporary deviations from the field's normal polarity, characterized by significant decreases in field intensity and magnetic poles wandering to lower latitudes without completing a full reversal (Buffett 2024; Constable and Morzfeld 2025). Finally, the model's occurrences of complete polarity flips, where most or all spins reverse polarity, correspond to geomagnetic reversals observed in the geological record (Valet *et al.*, 2005; Valet and Fournier 2016; Constable and Morzfeld 2025).

The random term in equation (3) is not essential for producing the mechanism observed in Figure 3, as this behavior arises from the inherent complexity of the equations themselves. Nakamichi *et al.*, (2012) analyzed cases in which both the random and drag terms were omitted, as well as a purely diffusive scenario. In the latter, the second time derivative in equation (3) becomes negligible, reducing the system to a set of first-order ordinary differential equations with random terms.

$$\frac{d\theta_i}{dt} = \gamma \sin 2\theta_i - \lambda \left[ \cos \theta_i (\sin \theta_{i-1} + \sin \theta_{i+1}) - \sin \theta_i (\cos \theta_{i-1} + \cos \theta_{i+1}) \right] + \frac{\epsilon \chi_i}{\sqrt{\tau}} \quad (4)$$

In these equations, the coefficient  $\kappa$  is absorbed by the other coefficients, thus reducing the total number of hyperparameters to four ( $N$  included). The values of parameters used in simulations changes and the exploration of the respective parameters' space remains a future venue of research. Solving these equations using the Runge-Kutta method is easier

and a typical realization (not shown here) is qualitatively similar to the one provided in Fig. 3.

The qualitative resemblance among these realizations is misleading. Nakamichi *et al.*, (2012) have suggested that the realizations of the domino model (3) and the diffusive version (4) are similar to each other. One simple and straightforward way to test this assertion is by calculating the ratio of the Probability Distribution Function (PDF) for each Axial Component series, generated by each version of the domino model (either 3 or 4). The PDFs have the same binning and we have opted for a smaller number of bins to avoid the effect of statistical fluctuations. If the models are similar to each other, the ratio for each bin should be close to one. The ratio plot in Fig. 4 shows that the PDFs of both models are quite different. Especially the central bins are distinctly further away from the similarity line (the reference level in the plot). Thus, we can state the presumed similarity between these models does not hold from a quantitative perspective. In reality, these models stand as two distinct ones.

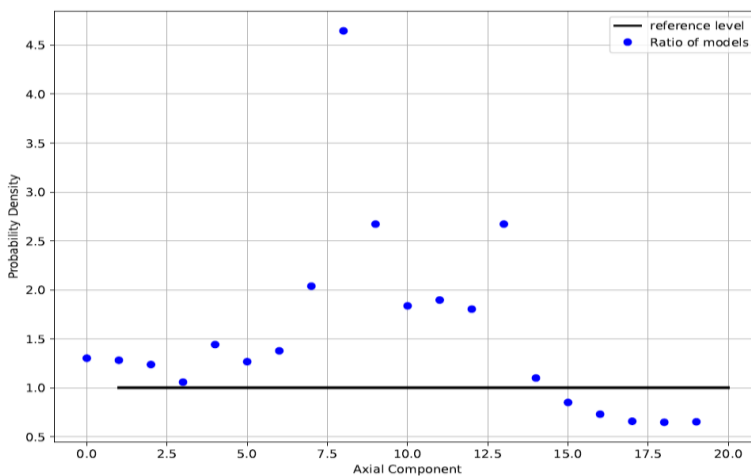


**Fig. 4.** Ratio plot of the PDFs of the domino models (4) and (5). The horizontal line that depicts the value 1 would be the case when the ratio of respective bins is 1. In this case, the PDF has 20 bins. Further increase to 50 bins does not improve the result suggesting essential differences between the models.

The discrepancy in the central bins indicates notable differences in how each model represents the Earth's magnetic field behavior. The central bins typically correspond to the most probable or average values of the geomagnetic dipole moment. Discrepancies here suggest that the models

differ in their portrayal of the Earth's typical magnetic field strength. As secular variation refers to the gradual change in the Earth's magnetic field over time, differences in the central bins may imply that the models have different sensitivities to these long-term changes. Furthermore, the central part of the distribution is influenced by the frequency and characteristics of geomagnetic excursions (temporary deviations) and reversals (polarity switches). Discrepancies here could indicate that the models differ in how they simulate these phenomena.

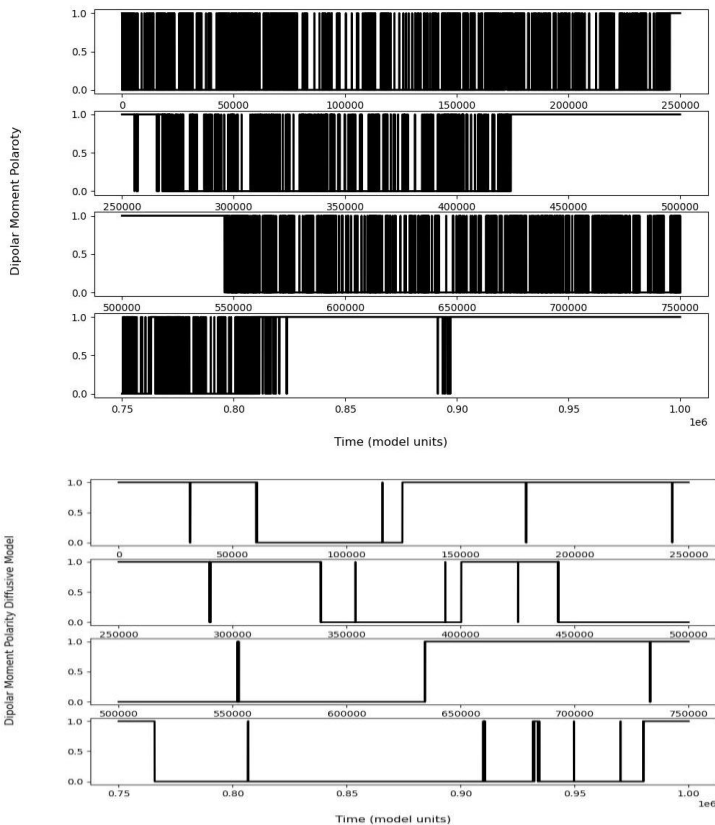


**Fig. 5** a) Time series of polarities (upper 4 panels) pertaining to a realization of the domino model (3). The graph shows the polarity and not the magnitude of the dipolar geomagnetic field. The color filling has been employed for clarity, where empty intervals represent normal polarity (current one), while filled intervals represent reverse polarity periods. b) Similar graph (lower 4 panels), but for the domino model (4). The color filling has not been employed because it is not needed.

Interestingly, the domino model (3) (Fig. 5, upper panel) qualitatively reproduces the observed pattern of geomagnetic reversals shown in Fig. 1. The model demonstrates intermittent polarity reversals of the dipolar geomagnetic moment, as well as variations in reversal frequency. The figure presents a portion of a long realization of the model, covering 50 million model time units. However, other realizations of the same model (not shown) exhibit similar behavior.

From a quantitative standpoint, the observed data set has been analyzed statistically by Ryan and Sarson (2007). They conducted statistical tests using 14 different distributions under the assumption that the time intervals between reversals are randomly distributed. Their analysis included two data sets, one of which originated from Cande and Kent (1992), yielding closely similar results. According to their findings, the best-fitting distributions are the 3-parameter log-logistic and 3-parameter lognormal distributions. Both are heavy-tailed, but with distinct tail shapes. The authors note that the log-logistic distribution does not treat the longest reversal-free period on record—the Cretaceous Normal Superchron—as an outlier, in contrast to the lognormal distribution. Given that the exact duration of the superchron remains uncertain, they also analyzed the data set without it, finding that the lognormal distribution provides the best fit in that case. Unfortunately, the authors do not report the specific parameter values for comparison. For the domino model (3), the best-fitting distribution is also lognormal, with parameters  $\mu = -1.27 \pm 0.02$  and  $\sigma = 0.99 \pm 0.04$ —values very close to those reported by Duka *et al.*, (2015):  $\mu = -1.29 \pm 0.03$  and  $\sigma = 0.97 \pm 0.02$ . In contrast, for domino model (4), the distribution deviates from lognormal and exhibits a heavier tail, indicating a higher number of long intervals between reversals.

Regarding domino model (3), we observe that long stretches of time without reversals occasionally occur, followed by periods characterized by frequent reversals. However, the distinct pattern of a decrease followed by an increase in reversal frequency—observed in the palaeomagnetic record—has not yet been reproduced. This raises at least two possibilities: either the current observations represent a limited snapshot of a much longer series encompassing the entire history of the Earth's magnetic field, within which reversal frequency changes randomly; or the geodynamo undergoes critical transitions that account for the observed variations in frequency (Raphaldini *et al.*, 2021). If the latter is true, it becomes essential to identify and investigate the mechanisms that drive such transitions. Our analysis thus far suggests that the inertial terms included in model (3)—

but absent in model (4)—are a crucial component in explaining changes in reversal frequency. For example, the reversal record generated by model (4) (Fig. 5, lower four panels) shows significantly fewer reversals and no evident variation in their frequency. However, these findings are not yet conclusive, as the behavior of both models is highly sensitive to parameter selection. Therefore, a more detailed and systematic analysis is required to obtain robust and generalizable results.

#### 4. Discussions: Further Extensions

Many magnetohydrodynamic (MHD) simulations have shown that the inner core and its magnetic moment significantly influence the geomagnetic reversal mechanism (Hollerbach and Jones 1993; 1995; Christensen and Wicht 2009; Davies *et al.*, 2013). It is generally believed that the inner core's induced magnetic moment helps stabilize the overall dipolar field, thereby suppressing strong variations and inhibiting reversals. Incorporating the solid inner core into the domino model may allow for the capture of its dynamic interactions with the fluid outer core. The inner core interacts with the outer core primarily through gravitational forces and electromagnetic coupling. These interactions influence the flow patterns in the outer core and, consequently, the process of geomagnetic field generation (Duan and Huang 2020). To incorporate the inner core's effects into the domino model, a central spin can be introduced to represent its magnetic contribution and dynamic behavior. This central spin would be coupled to the surrounding spins, simulating its stabilizing influence on the system.

To enhance the realism of the domino model and explore phenomena associated with the turbulent environment of the Earth's outer core, it is necessary to incorporate the effects of turbulence (Schaeffer *et al.*, 2017). Although complex, this task is essential for a deeper understanding of geomagnetic behavior, including the occurrence of geomagnetic reversals. Turbulence is inherently difficult to model due to its chaotic and stochastic nature, characterized by irregular fluid motions and fluctuations (Buffett 2014). There are several promising approaches for incorporating turbulence into the domino model. One straightforward method is to introduce stochastic perturbations in the coupling strengths between spins. Turbulent flows in the outer core cause random fluctuations in fluid motion, which in turn can modulate the interactions between adjacent spins. By including stochastic terms to randomize these coupling strengths,

we can simulate the influence of turbulence in a simplified manner. A more sophisticated approach involves coupling the domino model to a shell model of turbulence (Ryan and Sarson 2007). Rather than directly altering the domino dynamics, the shell model captures the energy cascade typical of turbulent flows—transferring kinetic energy from large to small scales. This coupling introduces time-dependent forcing into the domino system based on the turbulent energy spectrum, providing a dynamic, multiscale framework that reflects more realistic core conditions. Another advanced technique is the inclusion of memory effects via fractional dynamics (Buffett *et al.*, 2013). Turbulent flows often exhibit long-range temporal correlations, meaning that past fluctuations influence future states. These memory effects can be modeled using fractional differential equations, where the tilt rate of a given spin depends not only on its current state but also on its past behavior—up to and including its full history in the most extreme cases.

As a final point, it is important to consider potential challenges when integrating stochastic ordinary differential equations (SODEs)—i.e., ODEs that include random terms. Classical numerical methods such as the Runge-Kutta scheme are designed for smooth, deterministic systems and assume continuous, differentiable evolution of the integrated function. In cases where the stochastic terms are modeled as white noise—representing uncorrelated random fluctuations—these methods often still yield reliable results without significant distortion (Nakamichi *et al.*, 2012; Mori *et al.*, 2013; Pegini *et al.*, 2015). However, caution is warranted when the stochastic terms deviate from white noise assumptions, especially in systems influenced by turbulence or colored noise, where correlations in time may play a significant role. To address such complexities, alternative numerical schemes better suited for stochastic systems have been developed and will be discussed in detail in a forthcoming paper. Among these, the Euler–Maruyama method serves as a foundational approach for numerically solving stochastic differential equations (Kloeden and Platen 1992). Another notable method is the Milstein scheme, which extends Euler–Maruyama by incorporating terms that account for the derivative of the diffusion coefficient. This makes the Milstein method particularly appropriate for systems influenced by turbulence, where the stochastic components exhibit more complex behavior.

## 5. CONCLUSIONS

Magnetic field reversals, as recorded in palaeomagnetic datasets, remain one of the most intriguing phenomena in geodynamo studies. Although many magnetohydrodynamic (MHD) simulations are capable of replicating these reversals (Schaeffer *et al.*, 2017), such models are computationally intensive and typically constrained to relatively short timescales. Consequently, they often fail to generate reversal records that are sufficiently long or detailed for robust statistical analysis (Olson *et al.*, 2010). Additionally, the inherent complexity of these simulations makes it difficult to isolate and understand the individual mechanisms driving the reversal process.

In contrast, the domino model offers notable advantages in terms of simplicity and computational efficiency. It is straightforward to construct, easy to modify, and well-suited for testing a wide range of hypotheses without the high resource demands of full MHD simulations. This flexibility makes it particularly valuable for investigating the statistical characteristics of geomagnetic reversals, transitions between active and quiescent regimes, and the underlying physical mechanisms. Notably, domino model (3) demonstrates a strong ability to qualitatively reproduce the observed reversal record, even without changing any of its parameters. However, further research is required to determine whether it provides a physically plausible explanation for the observed behavior.

Looking forward, the domino model holds significant promise as an intermediary between theoretical analysis and large-scale numerical simulations. By incorporating more realistic representations of turbulence—particularly those reflecting the dynamic conditions in Earth's outer core—the model can be progressively enhanced to include key physical processes currently absent. This iterative approach not only facilitates deeper insight into the physics of magnetic reversals but also supports the refinement of more comprehensive MHD models. As such, the domino model may evolve into a practical and insightful tool for both exploring theoretical concepts and guiding future geodynamo research.

## ACKNOWLEDGEMENTS

We gratefully acknowledge the use of the HPC Cluster acquired through the project “Ngritja e një qendre llogaritëse në mbështetje të bashkëpunimit të IAL-ve shqiptare me projektin european *Compact Muon*

*Solenoid (CMS) në CERN,*” funded by AKKSHI. We declare no competing interests related to the content of this paper.

Additionally, anyone interested in further technical details is welcome to contact the author directly.

## REFERENCES

- Backus G, Constable C, Parker R. 1996.** Foundations of Geomagnetism. New York, NY: Cambridge University Press.
- Buffett BA, Ziegler L, Constable CG. 2013.** A stochastic model for palaeomagnetic field variations. *Geophysics Journal International*, **195**: 86–97. doi: 10.1093/gji/ggt218.
- Buffett BA. 2014.** Geomagnetic fluctuations reveal stable stratification at the top of the Earth's core. *Nature*, **507(7493)**: 484-7. PMID: 24670768 DOI: [10.1038/nature13122](https://doi.org/10.1038/nature13122).
- Buffett BA. 2024.** Excursions, reversals, and secular variation: Different expressions of a common mechanism? *Geochemistry, Geophysics, Geosystems*, 25 e2024GC011604: 1-17. <https://doi.org/10.1029/2024GC011604>.
- Busse FH. 1975.** Patterns of convection in spherical shells. *Journal of Fluid Mechanisms*, **72(1)**: 67 – 85. <https://doi.org/10.1017/S0022112075002947>.
- Cande SC, Kent DV.1992.** A new geomagnetic polarity time scale for the late Cretaceous and Cenozoic. *Journal of Geophysical Research*, **97 (B10)**: 13917–13951. <https://doi.org/10.1029/92JB01202>.
- Carbone V, Alberti T, Lepreti F, Vecchio A. 2020.** A model for the geomagnetic field reversal rate and constraints on the heat flux variations at the core-mantle boundary. *Scientific Reports*, **10 (13008)**: <https://doi.org/10.1038/s41598-020-69916-w>.
- Constable C, Morzfeld M. 2025.** Weather at the core: defining and categorizing geomagnetic excursions and reversals. *Geophysical Journal International*, **240 (1)**: 747–762. <https://doi.org/10.1093/gji/ggae415>.
- Davidson PA. 2013a.** Scaling laws for planetary dynamos. *Geophysical Journal International*, **195 (1)**: 67-74. [10.1093/gji/ggt167](https://doi.org/10.1093/gji/ggt167), [10.48550/arXiv.1302.7140](https://arxiv.org/abs/10.48550/arXiv.1302.7140).

- Davidson PA. 2013b.** Turbulence in rotating, stratified and electrically conducting fluids. Cambridge University Press. Online ISBN 781139208673 DOI: <https://doi.org/10.1017/CBO9781139208673>.
- Davies CJ, Silva L, Mound J. 2013.** On the influence of a translating inner core in models of outer core convection. *Physics of the Earth and Planetary Interiors*, **214**: 104–114. DOI:[10.1016/j.pepi.2012.10.001](https://doi.org/10.1016/j.pepi.2012.10.001).
- Duan P, Huang C. 2020.** On the mantle-inner core gravitational oscillation under the action of the electromagnetic coupling effects. *Journal of Geophysical Research: Solid Earth*, **125** (2): e2019JB018863. <https://doi.org/10.1029/2019JB018863>.
- Duka B, Peqini K, De Santis A, Francisco-Carrasco JP. 2015.** Using domino model to study the secular variation of the geomagnetic dipolar moment. *Physics of Earth and Planetary Interiors*, **242**: 9-23. DOI:[10.1016/J.PEPI.2015.03.001](https://doi.org/10.1016/J.PEPI.2015.03.001).
- Guyodo Y, Valet JP. 2006.** A comparison of relative paleointensity records of the Matuyama Chron for the period 0.75-1.25 Ma. *Physics of the Earth and Planetary Interiors*, **156** (3-4): 205–212. <https://doi.org/10.1016/j.pepi.2005.03.020>.
- Hollerbach R, Jones CA. 1993.** Influence of the Earth's inner core on geomagnetic fluctuations and reversals. *Nature*, **365**: 541–543. <https://doi.org/10.1038/365541a0>.
- Hollerbach R, Jones CA. 1995.** On the magnetically stabilizing role of the Earth's inner core. *Physics of the Earth and Planetary Interiors*, **87** (3-4): 171–181.
- Kageyama A, Sato T. 1997.** Velocity and magnetic field structures in a magnetohydrodynamic dynamo. *Physics of Plasmas*, **4** (5): 1569–1575. <https://doi.org/10.1063/1.872287>.
- Kloeden PE, Platen E. 1992.** Numerical Solution of Stochastic Differential Equations. Springer-Verlag, Berlin.
- Kuipers J, Hoyng P, Wicht J, Barkema GT. 2009.** Analysis of the variability of the axial dipole moment of a numerical geodynamo model. *Physics of Earth and Planetary Interiors*, **173**(3-4): 228–232. <https://doi.org/10.1016/j.pepi.2008.12.001>.
- Mori N, Schmitt D, Wicht J, Ferriz-Mas A, Mouri H, Nakamichi A, Morikawa M. 2013.** Domino model for geomagnetic field reversals. *Physical Review E* **87**: 012108. DOI: <https://doi.org/10.1103/PhysRevE.87.012108>.

- Nakamichi A, Mouri H, Schmitt D, Ferriz-Mas A, Wicht J, Morikawa M. 2012.** Coupled spin models for magnetic variation of planets and stars. *Monthly Notices of the Royal Astronomical Society*, **423 (4)**: 2977–2990.  
<https://doi.org/10.1111/j.1365-2966.2012.20862.x>.
- Olson PL, Coe RS, Driscoll PE, Glatzmaier GA, Roberts PH. 2010.** Geodynamo reversal frequency and heterogeneous core-mantle boundary heat flow. *Physics of Earth and Planetary Interiors*, **180 (1-2)**: 66–79. [10.1016/j.pepi.2010.02.010](https://doi.org/10.1016/j.pepi.2010.02.010).
- Olson PL, Deguen R, Hinnov LA, Zhong Sh. 2013.** Controls on geomagnetic reversals and core evolution by mantle convection in the Phanerozoic. *Physics Earth Planetary Interiors*, **214**: 87-103.  
<https://doi.org/10.1016/j.pepi.2012.10.003>
- Olson PL, Hinnov LA, Driscoll PE. 2014.** Nonrandom geomagnetic reversal times and geodynamo evolution. *Earth and Planetary Science Letters*, **388**: 9-17.  
<https://doi.org/10.1016/j.epsl.2013.11.038>.
- Peqini K, Duka B, De Santis A. 2015.** Insights into pre-reversal paleosecular variation from stochastic models. *Frontiers in Earth Science*, **3 (52)**: 1-13.  
<https://doi.org/10.3389/feart.2015.00052>.
- Peqini K, Koçi E, Prenga D, Osmanaj R. 2023.** The Core-Mantle boundary velocity field in the recent decades. *AIP Conference Proceedings*, **2872**, 120063. <https://doi.org/10.1063/5.0162927>.
- Raphaldini B, Medeiros ED, Ciro D, Franco DR, Trindade RIF. 2021.** Geomagnetic reversals at the edge of regularity. *Physical Review Research*, **3**: 013158.  
<https://doi.org/10.1103/PhysRevResearch.3.013158>.
- Roberts PH, King EM. 2013.** On the genesis of the Earth's magnetism. *Reports on Progress in Physics*, **76**: 096801.  
<https://doi.org/10.1088/0034-4885/76/9/096801>.
- Ryan DA, Sarson GR. 2007.** Are geomagnetic field reversals controlled by turbulence within the Earth's core? *Geophysical Research Letters*, **34 (2)**: <https://doi.org/10.1029/2006GL028291>.
- Schaeffer N, Jault D, Nataf HC, Fournier A. 2017.** Turbulent geodynamo simulations: A leap towards earth's core. *Geophysics Journal International*, **211 (1)**: 1–29.

- Spence EJ, Nornberg MD, Jacobson CM, Parada C, Forest CB. 2006.** Observation of a Turbulent Plasma Dynamo. *Physical Review Letters*, **96 (5):** 055002. <https://doi.org/10.1103/PhysRevLett.96.055002>.
- Valet JP, Fournier A. 2016.** Deciphering records of geomagnetic reversals. *Rev. Geophys.* **54 (2):** 410–446. [10.1002/2015RG000506](https://doi.org/10.1002/2015RG000506).
- Valet JP, Meynadier M, Guyodo Y. 2005.** Geomagnetic dipole strength and reversal rate over the past two million years. *Nature*, **435:**802–805. doi: 10.1038/nature03674.